A Vision-Based Approach to Extracting the Tilt Angle and Altitude of a PTZ Camera

I-Hsien Chen* and Sheng-Jyh Wang

Department of Electronics Engineering, Institute of Electronics, National Chiao Tung University, 1001 Ta-Hsueh Road, Hsinchu, 300 Taiwan, R.O.C.

ABSTRACT

In this paper, the relationship between the tilt angle and altitude of a PTZ camera and the 3D-to-2D coordinate transformation is built. A vision-based approach is then proposed to accomplish the estimation of tilt angle and altitude based on the observation of some simple objects lying on a horizontal plane, with known intrinsic parameters of the PTZ camera. The patterns could be a circle, a corner with known angle, more than two corners with unknown but equal angles, or more than two line segments with unknown but equal lengths. Furthermore, if we are given a few line segments with known but not necessarily equal length, the estimation of tilt angle and altitude can also be achieved via an optimization procedure. The impacts of parameter fluctuations are analyzed via computer simulations. Experimental results on real images conform to our analysis and demonstrate the efficiency of this approach.

Keywords: Camera calibration, PTZ camera, surveillance

1. INTRODUCTION

PTZ (Pan-tilt-zoom) cameras are commonly used in surveillance systems for active monitoring. Even though the use of PTZ cameras provides the capability to dynamically follow monitored objects, the calibration of PTZ camera's extrinsic parameters is inherently a difficult problem. For static cameras, various kinds of approaches[1-5] have already been developed to calibrate camera's intrinsic and extrinsic parameters. On the other hand, some other techniques[6-8] calibrate camera's intrinsic parameters based on the movement of camera. However, for a video surveillance system with active cameras, camera's extrinsic parameters may vary all the time while a camera is under panning or tilting. If we want to dynamically follow the change of camera parameters while a PTZ camera is under panning or tilting, it would be impractical to repeatedly perform camera calibration based on these elaborate calibration processes.

For a PTZ camera, its pan angle and tilt angle implicate the distance from the camera to the field of view. Whenever there is a change in pan angle or tilt angle, the position, orientation, and shape of the projected objects may change accordingly. In this paper, we focus on the estimation of tilt angle. The motivation of this paper originated from the observation that people could usually make a rough estimate about the tilt angle of the camera simply based on some clues revealed in the captured images. For example, with the image shown in Figure 8(a), with the shape of the table and the two A4 papers on the table, we can easily infer that the camera has a pretty large tilt angle, which is expected to be larger than 45 degrees.

In this paper, we'll propose a vision-based approach to infer the tilt angle and altitude of a PTZ camera. This method does not need a large amount of data. It leads to low computational load and has the potential to be applied for dynamic camera calibration or for surveillance systems with multiple PTZ cameras. Here, we'll first deduce the 3D-to-2D coordinate transformation in terms of the tilt angle and altitude of a PTZ camera. Although a similar scene model[9] based on pan angle and tilt angle has been established, in this paper, we'll deduce a more complete formula that takes into account not only the translation effect but also the rotation effect when a PTZ camera is under a pure tilt movement. After having established the 3D-to-2D transformation, we'll propose an efficient method to infer both the tilt angle and altitude of a PTZ camera based on the observation of some simple objects lying on a horizontal plane. The objects could be a circle, a corner with known angle, more than two corners with unknown but equal angles, or more than two line segments with unknown but equal lengths. In comparison, an approach[10] recovered the transformation between the image and the ground plane to find the look-down angle. In the method, however, the height information of the observed object has to be known. In comparison, the height is not a necessity in our approach.

*kace.ee89g@nctu.edu.tw; phone 886-3-5712121-54177; fax 886-3-5731791

This paper is organized as follows. First, the camera model of our system and the 3D-to-2D transformation in terms of tilt angle are to be described in Section 2. In Section 3, we'll develop the mapping between the 3-D space and the 2-D image plane, under the constraint that all observed points are locating on a horizontal plane. Based on the back projection formula, the tilt angle and altitude of the camera can be estimated by viewing some simple patterns on a horizontal plane. Then, in Section 4, the sensitivity analysis with respect to parameter fluctuations will be discussed. Finally, experimental results over real data are demonstrated to illustrate the efficiency of this method.

2. BASIC EQUATIONS

2.1 Scene model

In the setup of our indoor surveillance system, a PTZ camera is mounted on the ceiling of our lab, about 3 meters above the ground plane. The lab is full of desks, chairs, PC computers, and monitors. This PTZ camera is allowed to pan, tilt, or zoom while it is monitoring the activities in the room. All the tabletops are roughly parallel to the ground plane. In this paper, we'll propose a simple method to estimate the tilt angle and altitude of the PTZ camera based on the captured images of a few corners with fixed angles or a few line segments with fixed length. These corners and line segments are to be placed on a horizontal plane. This method can be easily carried out by placing a few sheets of A4 paper on a tabletop, as shown in Figure 8(a). An A4 paper has four right-angle corners and its length and width are 297 mm and 210 mm, respectively. Based on this simple setup, we'll demonstrate that the tilt angle and altitude of the PTZ camera can be easily estimated. Figure 1 illustrates the modeling of such a camera setup. Here, we assume the observed objects locate on a horizontal plane $\prod$, while the PTZ camera lies with a height h above $\prod$. The PTZ camera may pan or tilt with respect to the rotation center O_R. Moreover, we assume the projection center of the camera, denoted as O_C, is away from O_R with distance r. To simplify the deduction of the following formulae, we define the origin of the rectified world coordinates to be the projection center O_C of a PTZ camera with zero tilt angle. The Z-axis of the world coordinates is along the optical axis of the camera, while the X- and Y-axis of the world coordinates are parallel to the x- and y-axis of the projected image plane, respectively, as shown in Figure 1. When the camera tilts, the projection center moves to O_C' and the projected image plane is changed to a new 2-D plane. In this case, the y-axis of the image plane is no longer parallel to the Y-axis of the world coordinates, while the x-axis is still parallel to the X-axis.
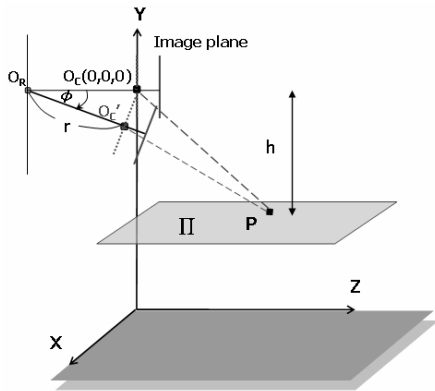

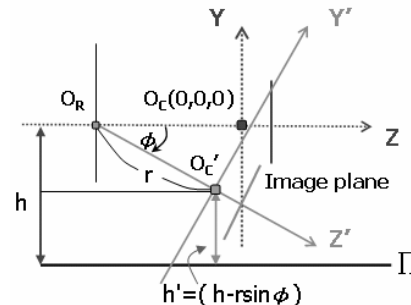
Figure 1: Model of camera setup.

Figure 2: Geometry of a horizontal plane with respect to a rectified camera and a tilted camera.

2.2 Coordinate mapping on a tilted camera

Assume $P=[X, Y, Z, 1]^T$ denotes the homogeneous coordinates of a 3-D point **p** in the world coordinates. For the case of a PTZ camera with zero tilt angle, we denote the perspective projection of **p** as $p= [x, y, 1]^T$. Under perspective projection, the relationship between P and p can be expressed as

$$p = \frac{1}{Z}\begin{bmatrix} \alpha & s & u_0 \\ 0 & \beta & v_0 \\ 0 & 0 & 1 \end{bmatrix}[R \quad t]P , \tag{1}$$

where α and β are the scale parameters expressed in pixel units for the x and y axes in the image plane, s is the skew factor due to some manufacturing error, and (u_0, v_0) is the principal point[11].

With respect to the rectified world coordinate system, the extrinsic term $[R\ t]$ becomes $[\mathbf{I}\ \mathbf{0}]$. To further simplify the mathematical deduction, we ignore the skew factor s and assume the image coordinates have been translated by a translation vector $(-u_0, -v_0)$. Hence, Equation (1) can be simplified as

$$\begin{bmatrix} x \\ y \\ 1 \end{bmatrix} = \frac{1}{Z} \begin{bmatrix} \alpha & 0 & 0 \\ 0 & \beta & 0 \\ 0 & 0 & 1 \end{bmatrix} \begin{bmatrix} X \\ Y \\ Z \end{bmatrix}. \tag{2}$$

or in a reverse way as

$$\begin{bmatrix} X \\ Y \\ Z \end{bmatrix} = Z \begin{bmatrix} \dfrac{1}{\alpha} & 0 & 0 \\ 0 & \dfrac{1}{\beta} & 0 \\ 0 & 0 & 1 \end{bmatrix} \begin{bmatrix} x \\ y \\ 1 \end{bmatrix} = \begin{bmatrix} \dfrac{xZ}{\alpha} \\ \dfrac{yZ}{\beta} \\ Z \end{bmatrix}. \tag{3}$$

When the PTZ camera tilts with an angle ϕ, the projection center O_C translates to a new place O_C' with $O_C' = [0\ -r\sin\phi\ -(r-r\cos\phi)]^T$. Assume we define a tilted world coordinate system (X', Y', Z') with respect to the tilted camera, with the origin being the new project center O_C', the Z'-axis being the optical axis of the tilted camera, and the X'- and Y'-axis being parallel to the x'- and y'-axis of the new projected image plane, respectively. Then, it can be easily deduced that in the tilted world coordinate system the coordinates of the 3-D point $\mathbf{p}$ become

$$\begin{bmatrix} X' \\ Y' \\ Z' \end{bmatrix} = \begin{bmatrix} 1 & 0 & 0 \\ 0 & \cos\phi & \sin\phi \\ 0 & -\sin\phi & \cos\phi \end{bmatrix} \begin{bmatrix} X \\ Y + r\sin\phi \\ Z + r(1 - \cos\phi) \end{bmatrix}$$
$$= \begin{bmatrix} X \\ Y\cos\phi + Z\sin\phi + r\sin\phi \\ -Y\sin\phi + Z\cos\phi + r(\cos\phi - 1) \end{bmatrix}. \tag{4}$$

Then, after applying the perspective projection formula, we know that the homogeneous coordinates of the projected image point now move to

$$\begin{bmatrix} x' \\ y' \\ 1 \end{bmatrix} = \begin{bmatrix} \alpha \dfrac{X'}{Z'} \\ \beta \dfrac{Y'}{Z'} \\ 1 \end{bmatrix} = \begin{bmatrix} \alpha \dfrac{X}{-Y\sin\phi + Z\cos\phi + r(\cos\phi - 1)} \\ \beta \dfrac{Y\cos\phi + Z\sin\phi + r\sin\phi}{-Y\sin\phi + Z\cos\phi + r(\cos\phi - 1)} \\ 1 \end{bmatrix}. \tag{5}$$

3. CONSTRAINED BACK-PROJECTIONS

3.1 Constrained coordinate mapping

In the rectified world coordinates, all points on a horizontal plane have the same Y coordinate. That is, $Y = -h$ for a constant h. The homogeneous form of this plane $\prod$ can be defined as $\pi = [0\ 1\ 0\ h]^T$. Assume the PTZ camera is tilted with an angle ϕ. Then, in the tilted world coordinate system, the homogeneous form of this plane $\prod$ becomes $\pi' = [0\ \cos\phi\ -\sin\phi\ (h - r\sin\phi)]^T$, as shown in Figure 2.

Assume a 3-D point $\mathbf{p}$ locates on the horizontal plane $\prod$. Then, in the rectified world coordinate system, we have $\pi \cdot P = 0$, where $P = [X, Y, Z, 1]^T$. Similarly, in the tilted world coordinate system, we have $\pi' \cdot P' = 0$, where $P' = [X', Y', Z', 1]^T$. With Equation (3), the constraint function becomes

$$\begin{bmatrix} 0 & \cos\phi & -\sin\phi & (h - r\sin\phi) \end{bmatrix} \begin{bmatrix} \dfrac{x'Z'}{\alpha} \\ \dfrac{y'Z'}{\beta} \\ Z' \\ 1 \end{bmatrix} = 0 \tag{6}$$

By solving (6), Z' is found to be

$$Z' = \frac{\beta(r\sin\phi - h)}{y'\cos\phi - \beta\sin\phi} . \tag{7}$$

Moreover, the tilted world coordinates of **p** become

$$\begin{bmatrix} X' \\ Y' \\ Z' \end{bmatrix} = \begin{bmatrix} \dfrac{x'\beta(r\sin\phi - h)}{\alpha(y'\cos\phi - \beta\sin\phi)} \\ \dfrac{y'(r\sin\phi - h)}{y'\cos\phi - \beta\sin\phi} \\ \dfrac{\beta(r\sin\phi - h)}{y'\cos\phi - \beta\sin\phi} \end{bmatrix} . \tag{8}$$

With Equations (4) and (8), we may transfer $[X', Y', Z']^{\mathrm{T}}$ back to $[X, Y, Z]^{\mathrm{T}}$ to obtain

$$\begin{bmatrix} X \\ Y \\ Z \end{bmatrix} = \begin{bmatrix} \dfrac{x'\beta(r\sin\phi - h)}{\alpha(y'\cos\phi - \beta\sin\phi)} \\ -h \\ \dfrac{(y'\sin\phi + \beta\cos\phi)(r\sin\phi - h)}{y'\cos\phi - \beta\sin\phi} - r + r\cos\phi \end{bmatrix} . \tag{9}$$

If the principal point is taken into account, then (9) can be reformulated as

$$\begin{bmatrix} X \\ Y \\ Z \end{bmatrix} = \begin{bmatrix} \dfrac{(x' - u_0)\beta(r\sin\phi - h)}{\alpha[(v_0 - y')\cos\phi - \beta\sin\phi]} \\ -h \\ \dfrac{[(v_0 - y')\sin\phi + \beta\cos\phi](r\sin\phi - h)}{(v_0 - y')\cos\phi - \beta\sin\phi} - r + r\cos\phi \end{bmatrix} . \tag{10}$$

This formula indicates the back projection formula from the image coordinates of a tilted camera to the rectified world coordinates, under the constraint that all the observed points are lying on a horizontal plane with $Y = -h$.

3.2 Pose estimation based on back-projections

In real life, based on the image contents of a captured image, people could usually have a rough estimate about the relative position of the camera with respect to the captured objects. In this section, we propose a simple method based on this observation. Here, we'll demonstrate that with a circle lying on a horizontal plane, we can easily estimate the tilt angle of the camera based on the back projection of the captured image. Similarly, we'll also demonstrate that the estimation of tilt angle is achievable based on the captured images of a few corners or a few line segments. Moreover, based on a few line segments with known lengths, not only the tilt angle but also the altitude of a PTZ camera can be extracted.

3.2.1 Back-projected circle w.r.t guessed tilt angle

Imagine we use a tilted camera to capture the image of a circle, which is locating on a horizontal plane. Based on the captured image and a guessed tilt angle, we may use (10) to back-project the captured image onto a horizontal plane on $Y = -h$. In Figure 3, we show the back-projected images for various choices of tilt angles. The original image is captured by a camera with $\phi = 16^{\circ}$. The choices of guessed tilt angles range from 0 to 30 degrees, with a 2-degree step. The back-projection for the choice of 16 degrees is plotted in bold font, especially. It can be seen that the back-projected image becomes a circle only if the guessed tilt angle is a correct one. That is, if the image of the circle is captured by a tilted camera with tilt angle ϕ, then the shape of the back-projection becomes a circle only when the guessed angle is equal to ϕ.
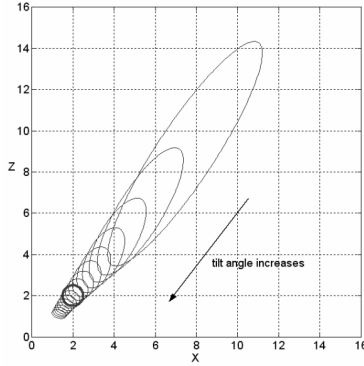
Figure 3: Illustration of back-projection onto a horizontal plane on $Y = -h$ for different choices of tilt angles.
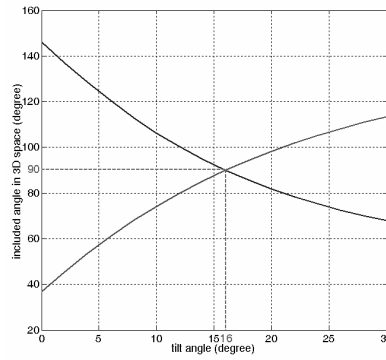
Figure 4: Illustration of the back-projected angle with respect to different choices of tilt angles.
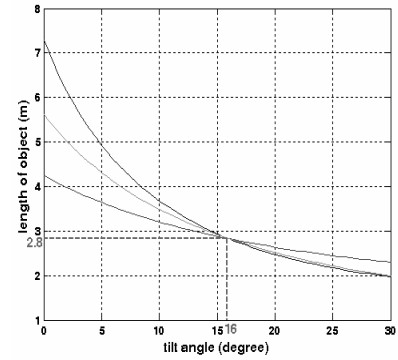
Figure 5: Illustration of the back-projected length with respect to different choices of tilt angles.

Otherwise, we'll get a distorted circle. It is also worth mentioning that a different choice of h only causes a scaling effect of the back-projected shape. The guessed tile angle still has to be the correct one no matter how we choose the value of h.

3.2.2 Back-projected angle w.r.t guessed tilt angle

The same phenomenon applies to corners with a fixed included angle. Assume three 3-D points, P_A, P_B, and P_C, on a horizontal plane form a corner at P_A with an angle ψ. The angle ψ can be calculated based on the following formula.

$$\cos\psi = \frac{\left\langle \overline{P_A P_B}, \overline{P_A P_C} \right\rangle}{\left\| \overline{P_A P_B} \right\| \times \left\| \overline{P_A P_C} \right\|} \tag{11}$$

After capturing the image of these three points, we can use their image coordinates and Equation (9) to build the relation between the back-projected angle and the guessed tilt angle.

$$
\begin{aligned}
\cos\psi = &\Big\{ \Big(\frac{x'_B \beta}{\alpha(y'_B \cos\phi - \beta\sin\phi)} - \frac{x'_A \beta}{\alpha(y'_A \cos\phi - \beta\sin\phi)} \Big) \\
&\times \Big(\frac{x'_C \beta}{\alpha(y'_C \cos\phi - \beta\sin\phi)} - \frac{x'_A \beta}{\alpha(y'_A \cos\phi - \beta\sin\phi)} \Big) \\
&+ \Big(\frac{(y'_B \sin\phi + \beta\cos\phi)}{y'_B \cos\phi - \beta\sin\phi} - \frac{(y'_A \sin\phi + \beta\cos\phi)}{y'_A \cos\phi - \beta\sin\phi} \Big) \\
&\times \Big(\frac{(y'_C \sin\phi + \beta\cos\phi)}{y'_C \cos\phi - \beta\sin\phi} - \frac{(y'_A \sin\phi + \beta\cos\phi)}{y'_A \cos\phi - \beta\sin\phi} \Big) \Big\} \\
&\times \Big\{ \Big(\frac{x'_B \beta}{\alpha(y'_B \cos\phi - \beta\sin\phi)} - \frac{x'_A \beta}{\alpha(y'_A \cos\phi - \beta\sin\phi)} \Big)^2 \\
&+ \Big(\frac{(y'_B \sin\phi + \beta\cos\phi)}{y'_B \cos\phi - \beta\sin\phi} - \frac{(y'_A \sin\phi + \beta\cos\phi)}{y'_A \cos\phi - \beta\sin\phi} \Big)^2 \Big\}^{-\frac{1}{2}} \\
&\times \Big\{ \Big(\frac{x'_C \beta}{\alpha(y'_C \cos\phi - \beta\sin\phi)} - \frac{x'_A \beta}{\alpha(y'_A \cos\phi - \beta\sin\phi)} \Big)^2 \\
&+ \Big(\frac{(y'_C \sin\phi + \beta\cos\phi)}{y'_C \cos\phi - \beta\sin\phi} - \frac{(y'_A \sin\phi + \beta\cos\phi)}{y'_A \cos\phi - \beta\sin\phi} \Big)^2 \Big\}^{-\frac{1}{2}}
\end{aligned}
\tag{12}
$$

Note that in (12) we have ignored the offset terms, u_0 and v_0, to reduce the complexity of the formulation.

In (12), the back-projected angle ψ doesn't depend on h and r. In Figure 4, we show the back-projected angle ψ with respect to the guessed tilt angle, assuming α and β are known in advance. In this simulation, we imagine there is a rectangular corner on a horizontal plane and we capture the image from a tilted camera with $\phi = 16$ degrees. Based on the captured image and a guessed tilt angle, we may back-project the corner image onto a horizontal plane in the 3-D space. With different choices of tilt angles, we get different back-projected angles. The two curves are generated by placing the rectangular corner on two different places of the horizontal plane. Again, the back-projected angle is equal to 90 degrees only if we choose the tilt angle to be 16 degrees. This means if we know in advance the angle of the captured corner, we can easily deduce camera's tilt angle based on (12). Moreover, the two curves intersect at $(\phi, \psi) = (16, 90)$. This means

that if we don't know the actual angle of the corner, we can simply place that corner on more than two different places of the horizontal plane. Then, based on the intersection of the deduced ψ -v.s.-ϕ curves, we may not only estimate the tilt angle of the camera but also the actual angle of the corner.

3.2.3 Back-projected length w.r.t. guessed tilt angle

Assume two 3-D points, P_A and P_B, on a horizontal plane form a line segment with length L. Similarly, we can build a similar relationship between the back-projected length and the guessed tilt angle by setting the constraint

$$\left\| \overline{P_A P_B} \right\| = L \, . \tag{13}$$

Based on (10) and (13), we can deduce that

$$
\begin{aligned}
L = \ell(\phi) = \{ & (\frac{(x'_B - u_0)\beta(r\sin\phi - h)}{\alpha[(v_0 - y'_B)\cos\phi - \beta\sin\phi]} \\
& - \frac{(x'_A - u_0)\beta(r\sin\phi - h)}{\alpha[(v_0 - y'_A)\cos\phi - \beta\sin\phi]})^2 \\
& + (\frac{[(v_0 - y'_B)\sin\phi + \beta\cos\phi](r\sin\phi - h)}{(v_0 - y'_B)\cos\phi - \beta\sin\phi} \\
& - \frac{[(v_0 - y'_A)\sin\phi + \beta\cos\phi](r\sin\phi - h)}{(v_0 - y'_A)\cos\phi - \beta\sin\phi})^2 \}^{\frac{1}{2}}
\end{aligned}
\tag{14}
$$

Similarly, if α, β, r, and h are known in advance, we can deduce the tilt angle directly based on the projected value of L.

Note that in (14), the right-side terms contain a common factor $(r\sin\phi{-}h)^2$. This means the values of r and h only affect the scaling of L. Hence, we can rewrite the formula of the L -v.s.-ϕ curve as

$$
\begin{aligned}
L' &\equiv \frac{L}{r\sin\phi - h} \\
&= [\left(\frac{(x'_B - u_0)\beta}{\alpha[(v_0 - y'_B)\cos\phi - \beta\sin\phi]} - \frac{(x'_A - u_0)\beta}{\alpha[(v_0 - y'_A)\cos\phi - \beta\sin\phi]} \right)^2 \\
&\quad + \left(\frac{[(v_0 - y'_B)\sin\phi + \beta\cos\phi]}{(v_0 - y'_B)\cos\phi - \beta\sin\phi} - \frac{[(v_0 - y'_A)\sin\phi + \beta\cos\phi]}{(v_0 - y'_A)\cos\phi - \beta\sin\phi} \right)^2]^{\frac{1}{2}}
\end{aligned}
\tag{15}
$$

Then, even if the values of r and h are unknown, we may simply place more than two line segments of the same length on different places of a horizontal plane and seek to find the intersection of these corresponding L -v.s.-ϕ curves, as shown in Figure 5. After the tilt angle estimation, based on (14), we can infer the altitude h with known length of L.

3.2.4 Estimation of tilt angle and altitude based on parameter optimization

We may also perform parameter estimation based on an optimization process. Here, we take (14) as an example to illustrate this procedure. We assume several line segments with known lengths (not necessary of the same length) are placed on different positions of a horizontal plane and we use a tilted camera to capture their picture. Assume the length of the ith segment is L_i, then we try to find a set of parameters $\{\alpha, \beta, u_0, v_0, \phi, r, h\}$ that minimize

$$F(\alpha, \beta, u_0, v_0, \phi, r, h) = \sum_{i=1}^{m} \left\| \ell_i(x'_i, y'_i, \alpha, \beta, u_0, v_0, \phi, r, h) - L_i \right\|^2 \, . \tag{16}$$

4. SENSITIVITY ANALYSIS AND EXPERIMENTS

In the formulae relating the back-projected angle and length with respect to the guessed tilt angle, several parameters tangle together in a fairly complicated way. In this section, we try to analyze how sensitive the estimation of tilt angle is with respect to parameter fluctuations. Finally, some experimental results over real data are demonstrated.

4.1. Sensitivity analysis

Ideally, when we place several corners or line segments on a horizontal plane, the deduced ψ -v.s.-ϕ curves or L -v.s.-ϕ curves should intersect at a single point. However, due to errors in the estimation of camera parameters, these curves usually do not intersect at a single point. Hence, in practice, we have to estimate the tilt angle based on the average of these intersection points. In this subsection, we'll discuss how parameter fluctuations affect the estimation of tilt angle.

Among these parameters, the distance r between the camera center and the rotation center has no impact over (12) and (15). Even in (14), r tends to have negligible impact since the term $r\sin\phi$ is usually much smaller than h. Hence, the parameter r can be ignored or be estimated via direct measurement. This means the parameters actually involved in the optimization of (16) can be reduced from 7 to 6. Moreover, in the following simulations, the images are assumed to be captured by a PTZ camera with tilt angle $\phi = 60$ degrees.

4.1.1 Sensitivity w.r.t. u_0 and v_0

As indicated in (10), the parameter u_0 only affects the numerate part of the back-projected X coordinate. Since the calculations of ψ and L depend on the distance between back-projected points, but not the absolute positions, this parameter has little impact over the deduced ψ -v.s.-ϕ curves and L -v.s.-ϕ curves. Based on Zhang's calibration method[2], the values of u_0 and v_0 are estimated to be 348 and 257, respectively. Even if the value of u_0 is changed by an amount of 100, the deduced tilt angle only changes about 0.1 degrees. On the other hand, the parameter v_0 has a larger but still acceptable impact over the estimation of tilt angle. As shown in Figure 6, a change of ±20 pixels in v_0 may cause a 1-degree deviation in the estimated tilt angle.
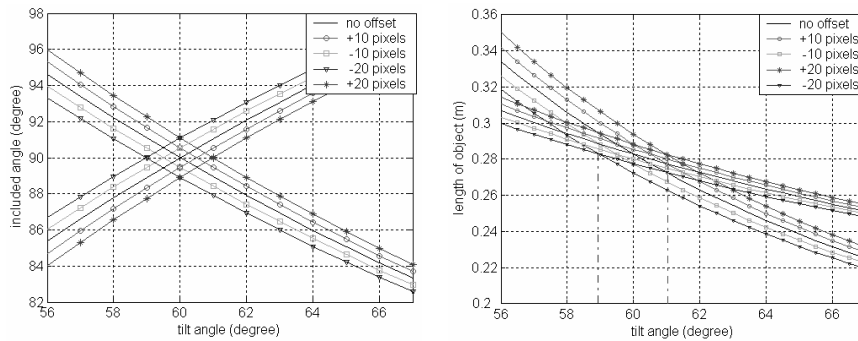

Figure 6: Sensitivity w.r.t. variation of v_0.

4.1.2 Sensitivity w.r.t. α and β

Similarly, the intrinsic parameters α and β also affects the estimation of tilt angle. Based on Zhang's calibration method[2], the values of α and β are estimated to be 770 and 750, respectively. As the value α is changed by the amount of ±20, the estimated tilt angle is found to have a ±1-degree fluctuation. Similarly, as the value β is changed by the amount of ±20, the estimated tilt angle is found to have a ±2-degree fluctuation. In Figure 7, we show how the fluctuation of β affects the estimation of tilt angle.
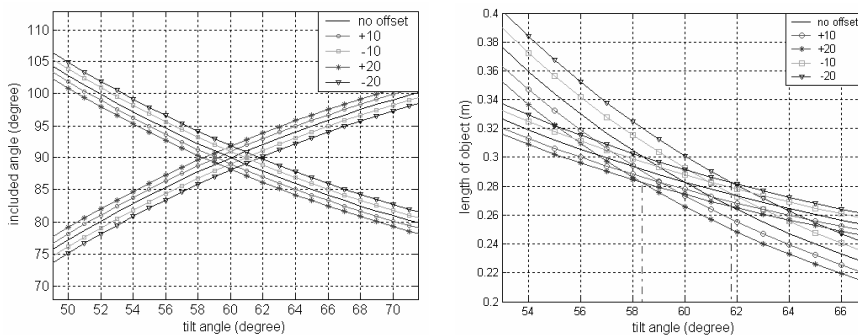

Figure 7: Sensitivity w.r.t. variation of β.

4.2. Experiments over real images

In the experiments over real images, the images are to be captured by a PTZ camera mounted on the ceiling with an unknown tilt angle. The image resolution is 640 pixels by 480 pixels. Two sheets of A4 paper are randomly placed on a horizontal table, as shown in Figure 8(a). The corners of these A4 paper sheets could be easily identified either by hand or by a corner detection algorithm. In the 3-D space, all the corners are 90 degrees, while the length and width of an A4 paper are 297 mm and 210 mm, respectively. In Figure 8(b) and (c), we show the deduced ψ -v.s.- ϕ curves and L -v.s.- ϕ curves based on the corners and the boundaries of these two A4 papers. The tilt angle is then estimated to be around 52 degrees. Note that there are two intersection points in Figure 8(c) whose vertical coordinate correspond to the length and width of an A4 paper, respectively.
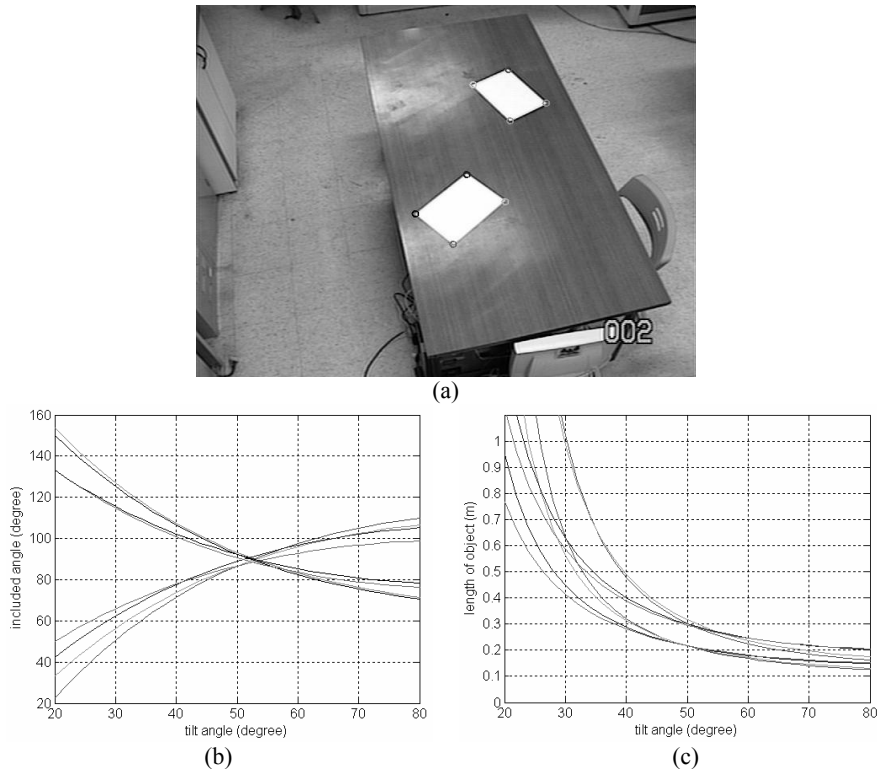

(a)

(b)   (c)

Figure 8: (a) Test image (b) Deduced ψ -v.s.- ϕ curves (c) Deduced L -v.s.- ϕ curves.

Table 1 and Table 2 list some experimental results based on the optimization of Equation (16). As mentioned above, the parameter r can be ignored and (16) includes only 6 unknown variables: α, β, u_0, v_0, ϕ and h. Similar to the setup shown in Figure 8(a), we randomly place a few A4 papers on a horizontal tabletop. In Table 1, each row corresponds to a different choice of initial conditions. For each choice of initial conditions, five observations are made with each observation includes 12 randomly selected line segments on the boundary of these A4 papers. Same as before, the lengths of these line segments would be either 297 mm or 210 mm. The mean and standard deviation of the estimated parameters are then calculated and listed in the last two columns of Table 1. It can be seen that, except u_0, all the estimated parameters have a quite small standard deviation. This fact indicates that a stable estimation about the tilt angle of a PTZ camera is achievable even if we choose the initial conditions to be quite different. The reason why u_0 has a larger standard deviation is caused by the fact that the projected segment length is less sensitive to u_0.

As shown in Figure 7, a larger value of β (or α) corresponds to a smaller value of tilt angle. The initial guess about the values of α and β does affect the estimation of tilt angle. In comparison, the initial guess about the values of ϕ and h would have less impact over the estimation of tilt angle and altitude. In Table 2, we perform another set of experiments, where the initial guess of $\{\alpha, \beta\}$ is chosen to be closer to $\{770, 750\}$, an estimation based on Zhang's calibration method[2]. It can be seen that in this case the estimation of tilt angle and h becomes even more stable. Moreover, these estimated intrinsic parameters are also very close to the results estimated by Zhang's method. This simulation result

indicates that if we could have a closer initial guess about α and β, we may achieve an even more stable estimation about both intrinsic and extrinsic parameters.

Table 1: Parameter estimation based on (16) with different initial conditions.

		Initial values of parameters		Mean		Deviation	
		650	650	682.21	627.75	3.33	2.25
		320	240	362.21	255.62	32.51	1.74
		45	1.5	57.19	1.87	0.72	0.02
		700	700	724.99	683.35	3.66	2.16
α	β	320	240	362.21	252.13	32.51	1.85
u0	v0	45	1.5	54.84	1.94	0.76	0.03
ϕ(degree)	h(m)	700	700	724.14	684.10	3.42	2.14
		320	240	362.21	252.30	32.51	1.81
		55	2	54.84	1.94	0.76	0.03
		750	750	764.96	740.72	4.21	2.87
		320	240	361.95	247.43	32.92	2.01
		45	1.5	52.41	1.99	1.04	0.04
Deviation				33.79	46.12		
				0.13	3.37		
				1.95	0.05		

Table 2: Parameter estimation based on (16) with the initial values of α and β close to the estimations by Zhang's method[2].

		Initial values of parameters		Mean		Deviation	
		750	760	768.99	748.42	4.34	2.70
		320	240	361.95	249.31	32.91	2.18
		45	1.5	52.18	1.99	1.04	0.04
		760	760	772.81	752.00	4.39	2.75
α	β	320	240	361.95	246.24	32.92	2.14
u0	v0	45	1.5	51.96	2.00	1.04	0.04
ϕ(degree)	h(m)	770	750	772.75	748.15	4.31	2.76
		320	240	361.95	241.43	32.92	2.16
		45	1.5	51.96	2.01	1.05	0.04
		780	740	773.00	744.67	4.27	2.70
		320	240	361.95	236.50	32.92	2.26
		45	1.5	51.95	2.02	1.05	0.04
Deviation				1.93	2.99		
				0.00	5.61		
				0.11	0.01		

ACKNOWLEDGEMENT

REFERENCES

1. Roger Y. Tsai, "A Versatile Camera Calibration Technique for High-Accuracy 3D Machine Vision Metrology Using Off-the-Shelf TV Cameras and Lenses", IEEE Journal of Robotics and Automation, **Volume: 3**, Issue: 4, pp. 323-344, Aug 1987.
2. Zhengyou Zhang, "Flexible Camera Calibration by Viewing a Plane from Unknown Orientations", The Proceedings of the Seventh IEEE International Conference on Computer Vision, **Volume: 1**, pages 666-673, Sept. 1999.
3. Zhengyou Zhang, "Camera Calibration with One-Dimensional Objects", IEEE Transactions on Pattern Analysis and Machine Intelligence, **Volume: 26**, Issue 7, pp. 892-899, July 2004.
4. Motilal Agrawal and Larry S. Davis, "Camera calibration using spheres: A semi-definite programming approach", In Proc. Ninth IEEE International Conference on Computer Vision, **Volume:.2**, pp. 782-789, Oct. 2003.
5. Guo-Qing Wei and Song De Ma, "A Complete Two-Plane Camera Calibration Method and Experimental Comparisons", In Proc. Fourth International Conference on Computer Vision, pp. 439-446, May 1993.
6. Robert T. Collins and Y. Tsin, "Calibration of an Outdoor Active Camera System", IEEE Computer Society Conference on Computer Vision and Pattern Recognition, **Volume: 1**, pp. 534, June 1999.
7. A. Basu and K. Ravi, **"**Active Camera Calibration Using Pan, Tilt and Roll", IEEE Transactions on Systems, Man and Cybernetics, Part B, **Volume: 27**, Issue: 3, pp. 559-566, June 1997.
8. Elsayed E. Hemayed, "A Survey of Camera Self-Calibration", In Proc. IEEE Conference on Advanced Video and Signal Based Surveillance, pp. 351-357, July 2003.
9. Ser-Nam Lim, L.S. Davis, and Ahmed Elgammal, "A Scalable Image-Based Multi-Camera Visual Surveillance System", In Proc. IEEE Conference on Advanced Video and Signal Based Surveillance, pp. 205-212, July 2003.
10. P. Remagnino and G.A. Jones, "Automated Registration of Surveillance Data for Multi-Camera Fusion", Proceedings of the Fifth International Conference on Information Fusion, **Volume: 2**, pp. 1190-1197, July 2002.
11. David A. Forsyth and Jean Ponce, *Computer Vision: A Modern Approach*, Prentice Hall, 2003.